Electronic Supplementary Information

Simulation of the self-assembly of simple molecular bricks into Sierpiński triangles

Damian Nieckarz and Paweł Szabelski

Department of Theoretical Chemistry, Maria-Curie SkłodowskaUniversity,
Pl. M.C. Skłodowskiej 3, 20-031 Lublin, Poland.

1. Details of the MC simulation

The simulation started with a mixture of N_m metal atoms and N_l randomly oriented linker molecules ($N_m + N_l = N$ in total) distributed on the triangular $L \times L$ lattice with $L = 200$. Next, one of the adsorbed species, *m* or *l*, was chosen at random and its potential energy in the old configuration, U_{old} was calculated. To that end, for each segment of the selected component (one for a metal atom) six neighboring sites were checked. If the neighboring site of the segment was occupied by the other component the potential energy was increased by ε, provided that the interaction occurred between the metal atom and the terminal segment of the linker oriented in such a way that the directional bond can be formed. In the remaining situations the contribution from the segment-segment interaction to U_{old} was equal to 0. Once the net potential energy U_{old} was summed out, an attempt was made to move the selected atom/linker molecule to a new randomly chosen position on the lattice. In the case of the linker molecule the displacement move was additionally accompanied by a random in-plane rotation of the backbone, by a multiple of 60 degrees. The selected atom/molecule was inserted in the new position only when the following conditions were fulfilled 1) the corresponding lattice sites in the new position were unoccupied and 2) the move did not involve the formation of a node in which the terminal linker segments occupy neighboring lattice sites at the perimeter of the metal atom. If it was the case, the energy of the metal atom/linker molecule in the new configuration, U_{new} was calculated using the same procedure, as described above for U_{old}. To decide whether the new configuration should be accepted or not, the acceptance probability $p = \min\{1, \exp[-(U_{new} - U_{old})/kT]\}$ was calculated and compared with a randomly generated number $r \in (0,1)$. If $r < p$ the new configuration was accepted; otherwise the move was rejected and the atom/molecule was left in the original position. During one MC step the above sequence was repeated *N* times, that is once per adsorbed entity on average. In the simulations we used typically up to 10^7 MC steps. To minimize the chances of the simulated system being trapped in metastable states the adlayer was equilibrated at $T = 1.0$ and next slowly cooled down to $T = 0.1$ at which the snapshots of the adsorbed structures were taken. The simulations were performed also at temperatures lower than 0.1 (see Fig. 3) but no further changes in the morphology of the adsorbed overlayers was observed. The annealing run consisted of 10^7 MC steps during which the initial temperature was linearly decreased from by 10^{-3} every 10^4 MC steps. The assumed density of the adsorbed phase, defined as fraction of occupied lattice sites (linker + metal), was chosen to be approximately the same for both molecules, that is 0.16 for **A** (1800 *l* + 1200 *m*) and 0.14 for the linker **B** (1200 *l* + 800 *m*).

The equilibrium MC simulation method used in this work allows for the spontaneous formation (assembly) and break-up (disassembly) of the 2D metal-organic aggregates through reversible metal-linker bonding. Unlike in irreversible models of aggregation, such as for example the diffusion limited aggregation (DLA)[1,2] model, the possibility of detachment of a linker molecule or a metal atom from the triangular aggregates is not *a priori* excluded in our case. As the self-assembly is controlled by temperature, the formation of the fractal patterns occurs at low values of $T < 0.2$ at which the formation of the 3-fold coordination nodes is largely enhanced (see Fig. 3) and the collapse of the aggregates occurs rarely. However, even under these conditions, which may seem close to irreversibility, there is still nonzero probability for the break-up of the linker-metal bond. This property makes the proposed model fundamentally different from the intrinsically irreversible models of self-assembly.

2. Structure formation in related systems

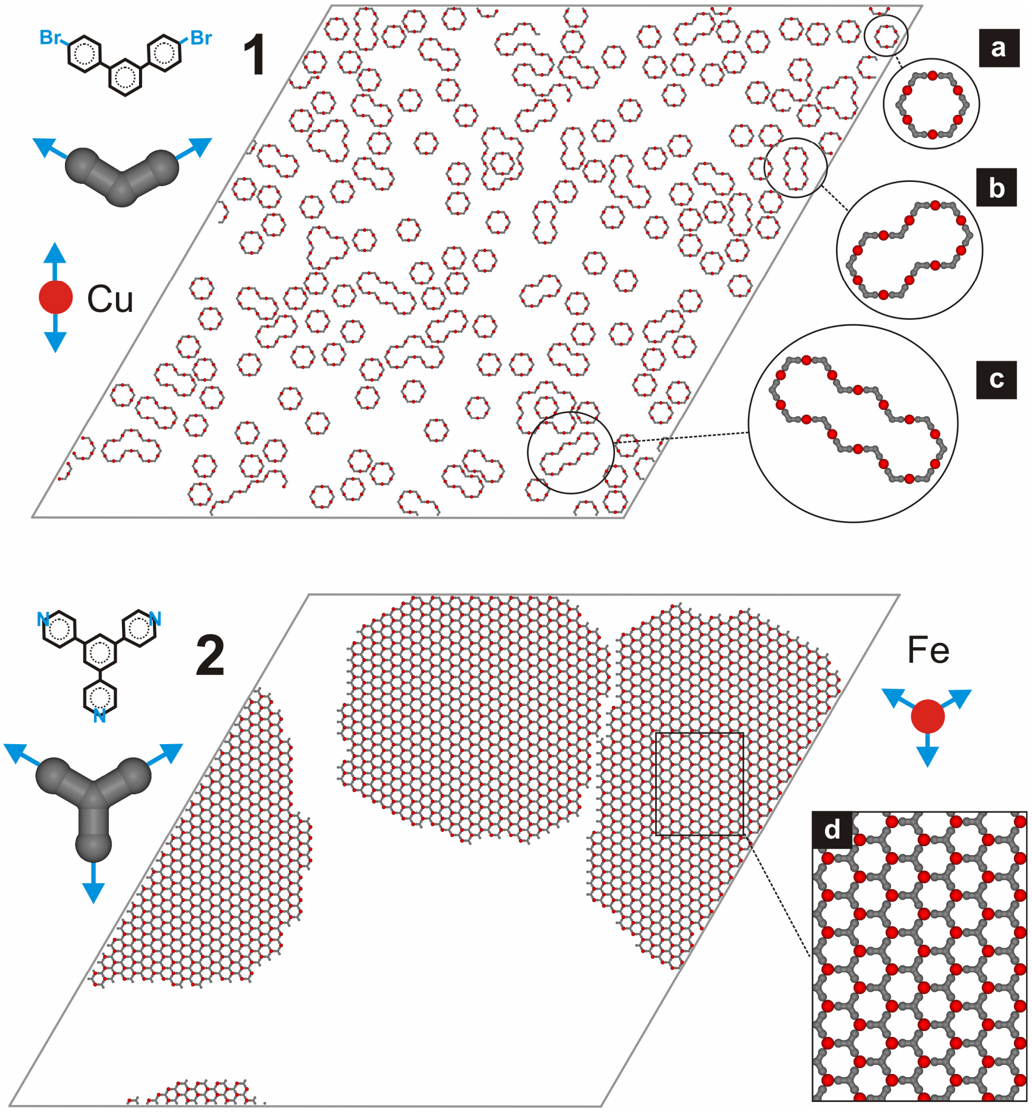

Figure S1. Representative results of the MC simulations performed for the experimentally relevant linkers **1** and **2** with structures similar to those assumed in this work.[6,7] In both cases the simulations were performed on a 200 by 200 triangular lattice using a suitably modified version of the algorithm described in the preceding section; $T = 0.1$, $\varepsilon = -1$. The blue arrows indicate the preferred interaction directions of each component. The top part corresponds to the formation of planar metal-organic macrocycles comprising meta terphenyl fragments and copper atoms observed during the Ullmann coupling of 4,4"-dibromo-*meta*-terphenyl on Cu(111);[7] 1000 molecules of **1** + 1000 Cu atoms. The magnified fragments (a), (b) and (c) are the hexamer and decamer and straight tetradecamer, respectively. The bottom part illustrates the self-assembly of 1,3,5-tri(4-pyridyl)-benzene and atomic iron co-deposited on Au(111) which has been reported by Shi and coworkers;[6] 2000 molecules of **2** + 2000 Fe atoms. The inset (d) is a magnified fragment of the metal-organic network with hexagonal pores. The structures shown in the figure are identical with their corresponding experimental counterparts.

3. Survey of the metal-linker coordination nodes

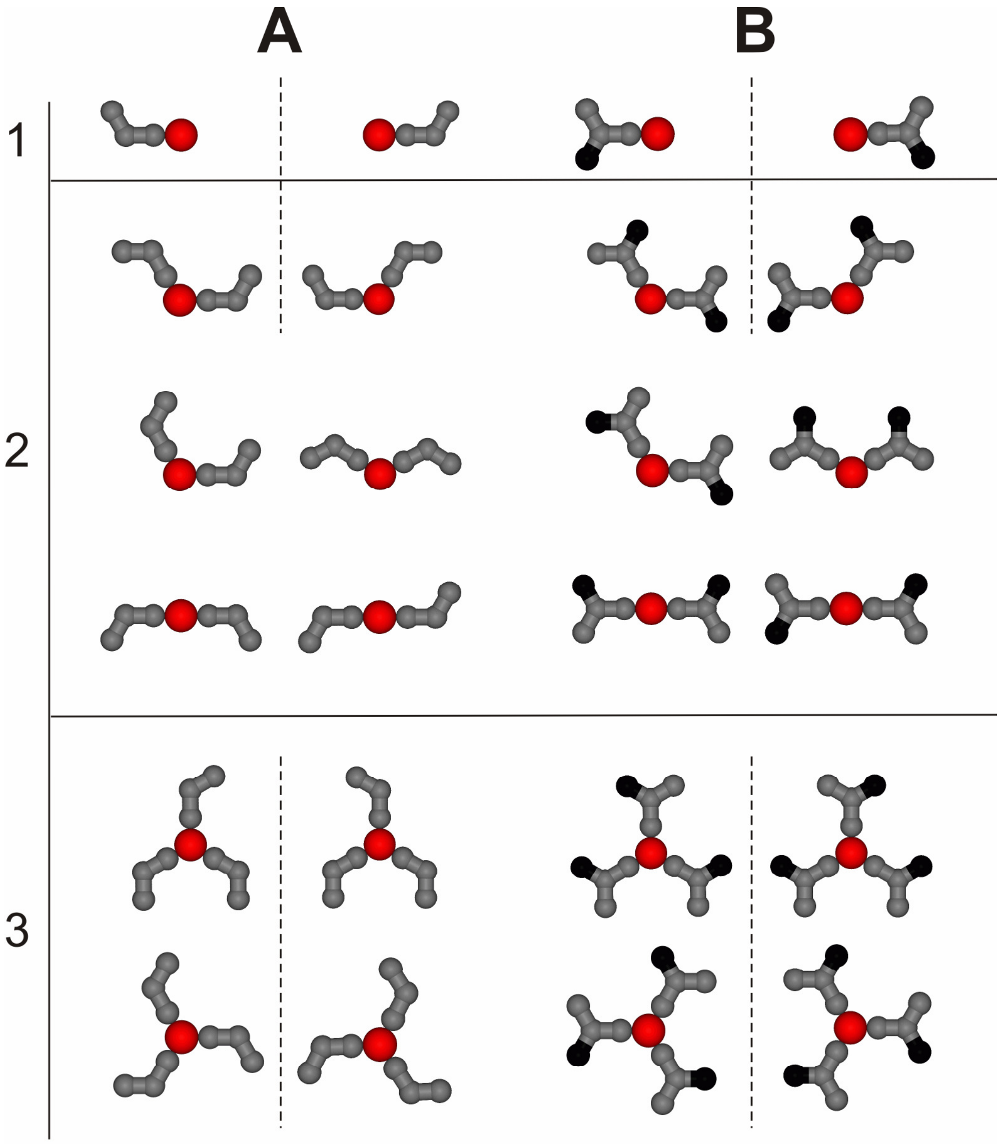

Figure S2. Possible metal-linker coordination nodes formed by the linker molecules **A** and **B** and the metal center whose coordination number is shown on the left. The dashed line represents the mirror plane. The inactive segment of linker **B** was colored in black.

3. Structural properties of the fractal aggregates

To demonstrate the relation between the classical Sierpiński triangle and the triangular aggregates obtained in the simulations in Fig. S2 we showed basic structural units of both architectures. For simplicity a linear linker molecule was used, able to form two collinear metal-organic bonds. This simplification alters only the topology of the coordination nodes, but it does not affect stoichiometry of the aggregates.

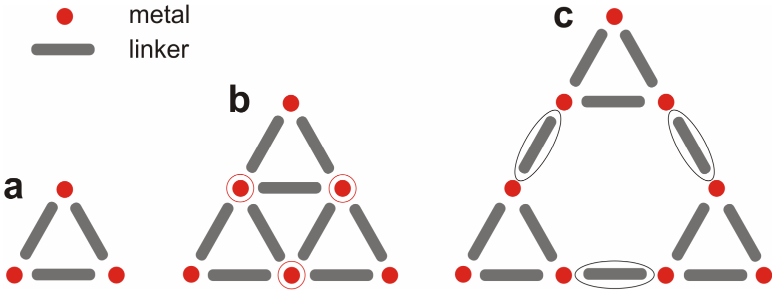

Figure S3. (a) Basic metal-organic triangular unit comprising three metal atoms and three linker molecules. (b) Connection of three units **a** through the common four-fold coordinated metal centers encircled in red. The resulting structure corresponds to the first generation of the classical Sierpiński triangle. (c) Connection of three units **a** through the additional linker molecules encircled in black. The structure **c** is a prototype of any Sierpiński-type triangular fractal comprising ditopic linker molecules and three-fold coordinated metal atoms.

The main structural difference between the Sierpiński triangle (b) and the triangle (c) is that these aggregates are sustained by nodes of a different connectivity, equal to three and four, respectively. Consequently, at the early stage of growth the linker-to-metal proportion in (c) is different from the corresponding ratio 3:2 calculated for the classical Sierpiński triangle from Fig.S2b and it equals to 4:3. As the structures (b) and (c) expand, the corresponding linker-to-metal proportions, x_b and x_c change and they approach 2 and 1.5, respectively according to the simple relations

$$x_b = \frac{2}{1+3^{-n}} \qquad \text{and} \qquad x_c = \frac{3}{2}\left(1 - \frac{1}{3^{n+1}}\right) \qquad (1)$$

where n is the generation of the triangular aggregate; $n=1$ for the triangles (b) and (c) from Fig. S2. The obtained limiting value of, $x_c = 1.5$ ($n \to \infty$) was used in our simulations as being optimal for the growth of large self-similar structures. To visualize the dependencies given by Eq. (1) in Fig. 3 we plotted the linker-to-metal ratio as a function of the generation number for (b) and (c).

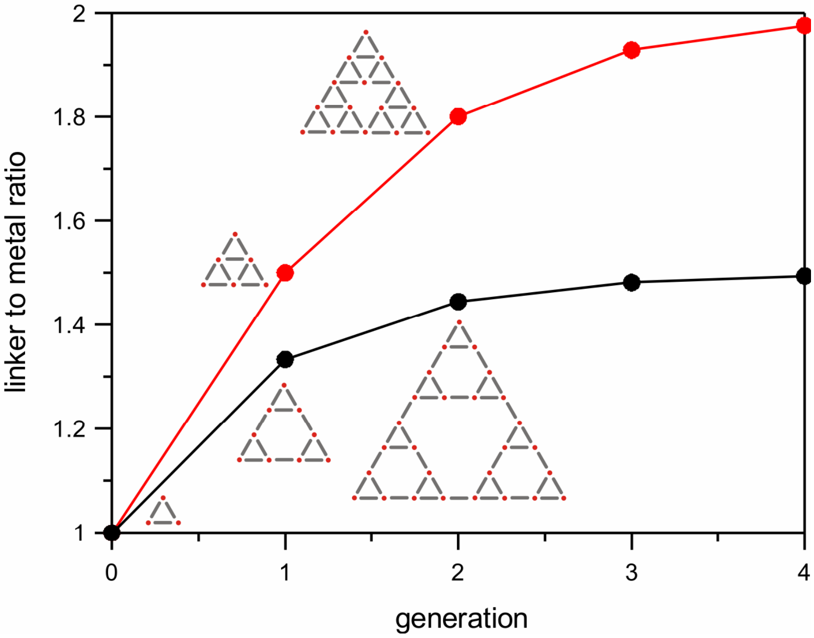

Fig. S4. Linker-to-metal ratio, x_b (red) and x_c (black) as a function of the generation number of the triangular metal-organic aggregate, n. The structures next to the datapoints are the corresponding generations of the aggregates sketched for $n \leq 2$.

4. Additional snapshots of the adsorbed overlayer

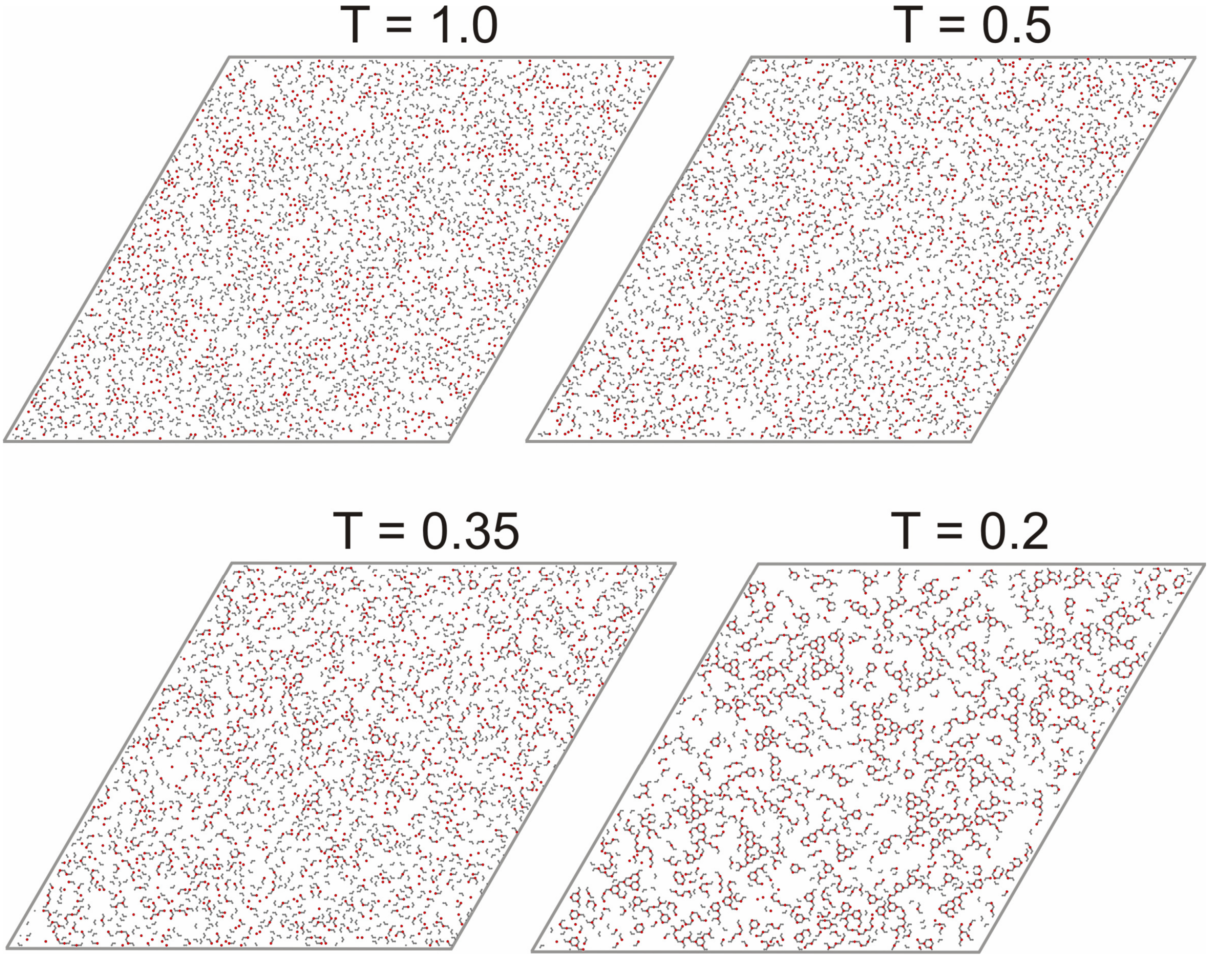

Figure S5. Snapshots of the adsorbed overlayer comprising 1800 molecules of **A** and 1200 metal atoms taken at the temperatures indicated by the black arrows in the left part of Fig. 3 and shown above each snapshot; $L=200$, $\varepsilon=-1$.

5. Examples of erroneous triangular structures

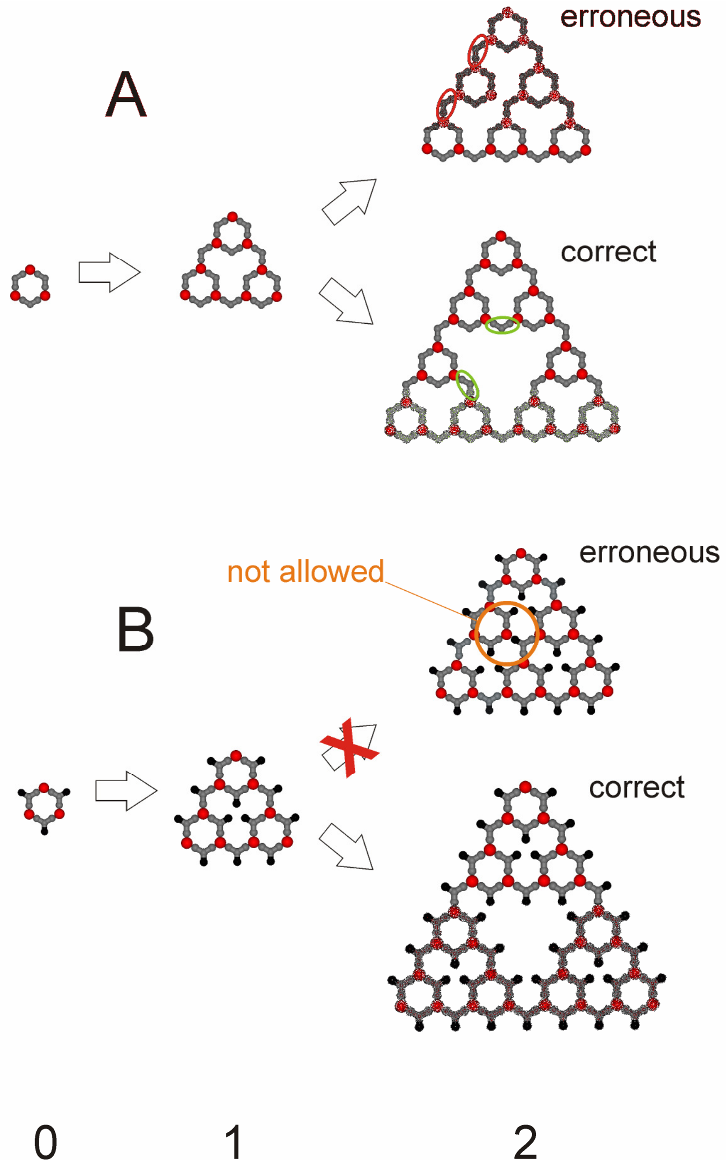

Figure S6. Hierarchical growth of the correct and erroneous triangular aggregates comprising molecules of **A** and **B**. The consecutive generations are described by the numbers in the bottom. For the linker **A** the exemplary erroneous structure is a result of the wrong orientation of the two linker molecules encircled in red. If these molecules are oriented properly (encircled in green) the triangle with correct geometry can be formed. For the linker **B** an analogous erroneous second-generation triangle cannot exist, as the metal-linker node encircled in orange is not allowed in the proposed model.